Electronic Supplementary Information

Title: Sustainable Conversion of Cellulosic Biomass to Chemicals under Visible-Light Irradiation

Lina Wang,[a] Zhanying Zhang,[b] Lixiong Zhang,[c] Song Xue,[d] William O. S. Doherty,[b] Ian M. O'Hara,[b] and Xuebin Ke*[a]

[a] *School of Chemistry, Physics and Mechanic Engineering, Queensland University of Technology. Brisbane, QLD 4101, Australia. Fax: +61 731381804; Tel:+ 61 731389197; E-mail: x.ke@qut.edu.au*

[b] *Centre for Tropical Crops and Biocommodities, Queensland University of Technology, 2 George Street, Brisbane, QLD 4001, Australia.*

[c] *State Key Laboratory of materials-oriented Chemical Engineering, College of Chemistry and Chemical Engineering, Nanjing University of Technology, Nanjing, China.*

[d] *School of Chemistry & Chemical Engineering, Tianjin University of Technology, Tianjin 300384, China.*

Experimental Details

Synthesis of zeolite Y and TiO_2 nanofibres. All chemicals used were purchased from Sigma-Aldrich. Zeolite Y and TiO_2 nanofibres were prepared by previously reported method in literature, [s1] and organic templates were removed by calcinations at 550 ^oC for 5 hours.

Preparation of Au-NPs loaded catalysts. Typically, 1.25 g of TiO_2 supported Y zeolites were dispersed into 50 mL of 3.8 mmol L^{-1} aqueous solution of chloroauric acid ($HAuCl_4$). Then 0.125 g of poly(vinyl alcohol) (PVA) was dispersed in 10 mL of deionised water, and was added into the mixture of solids and $HAuCl_4$ solution under stirring for 0.5 h.

To this suspension, 0.5 mL of 0.38 mol L^{-1} aqueous solution of tetrakis-(hydroxymethyl)phosphonium chloride (THPC, the reducing agent) was added dropwise, followed by adding 2.2 mL of 0.38 mol L^{-1} sodium hydroxide aqueous solution (NaOH). The mixture was stirred continuously for 2 h and aged statically for 24 h. Finally, the solid was washed with deionised water three times and ethanol once; and the obtained solids by centrifugation were dried at 60 °C for 16 h.

Preparation of H-form catalysts. Typically zeolite Y was ion-exchanged at 90 ^{o}C for 3 h for each run, under continuous stirring with 0.1 mol L^{-1} NH_4NO_3 aqueous solution to prepare HY. After each run of ion-exchange, the samples were washed and centrifuged thoroughly with deionised water and then calcinations were conducted at 400^{o}C for 3 hours. The 0.1 mol L^{-1} hydrochloric acid (HCl) aqueous solution was used to treat TiO_2 nanofibres. The dried solids after centrifugation were used directly as photocatalysts.

Characterisation of catalysts. XRD (X-ray Diffraction) patterns were obtained on the Philips PANalytical X'Pert PRO diffractometer, using Cu *Ka* radiation (λ=1.5418 Å) at 40 kV and 40 mA. The diffraction data were collected from 5^{o} to 75^{o} with a resolution of 0.01^{o} (2θ). UV/Vis spectra were recorded on the Cary 5000 UV/Vis-Nir Spectrophotometer, using light source of (200-800) nm in wavelength. The field emission scanning electron microscopy (FESEM, JEOL JSM-7001f) was utilized to observe the surface morphology of samples. The content of gold on a catalyst as well as Si/Al ratio in zeolites were determined by attached energy-dispersive X-ray spectroscopy (EDS).

Catalytic test. All the raw chemicals were purchased from Sigma-Aldrich and used without further treatment, including microcrystalline cellulose (powder, 50 Micron Avicel® PH-101 Fluka), 1-ethyl-3-methylimidazolium chloride (EMIMCl). Cellulose conversion experiments were carried out in a round-bottomed 50-mL transparent glass flask equipped

with a sealed spigot and a magnetic stirrer. As for a typical batch reaction, 50 mg cellulose was added into 4.5 g EMIMCl solution and stirred at 300 rpm for 1 hour at 130 °C to dissolve the cellulose, then 50 mg catalyst was charged into the flask, followed by adding 500 mg water. The reactor was exposed under visible light irradiation. The reaction temperature was controlled in the silicone oil bath. If without oil bath heating (only with light irradiation), the temperature can be up to 90 °C in two hours.

The flask was irradiated with a 500-Walt Halogen lamp, and the UV light was removed by using a glass filter to cut off the light with the wavelength shorter than 400 nm. The light intensity was controlled from 0 (light off) to 0.7 W cm^{-2}. Control experiments were performed without light irradiation, maintaining the other conditions identical. Aliquots (around 0.1 g) were collected at given time intervals. The samples were diluted 10 times with deionised water and filtrated through a Millipore filter (pore size 0.45 μm). The filtrates were analysed by a Waters high performance liquid chromatography system (HPLC, Bio-Rad Aminex 87 H column and a Waters refractive index detector). The mobile phase was 5 mM H_2SO_4 aqueous solution at a flow rate of 0.6 mL min^{-1}. The temperature for the column was 65 °C. The calculated yield (%) is the value of moles of the products determined by HPLC dividing moles of anhydroglucose units in cellulose.

Section 1: Product distributions for cellulose conversion varying with light intensity.

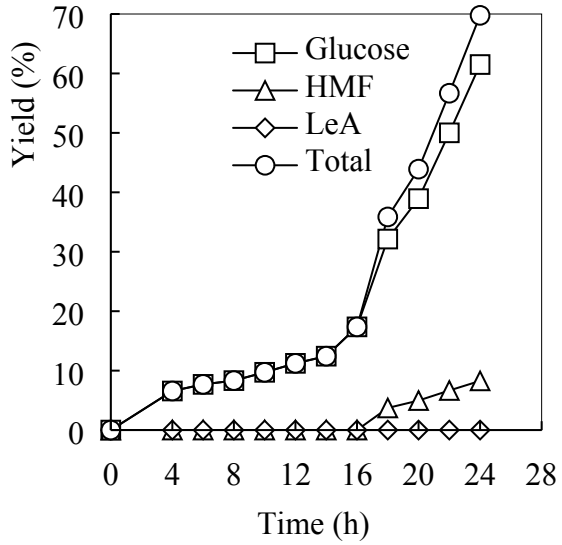

Fig. S1 The product distributions for cellulose conversion at light intensity of 0.7 W cm^{-2} at 130 °C.

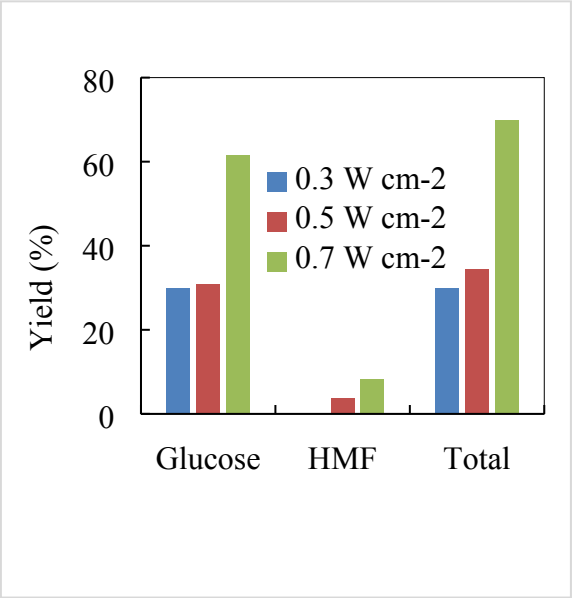

Fig. S2 The yields of valuable chemicals for cellulose conversion varying with light intensity at 24 hours.

Figure S1 illustrated the yields of valuable chemicals for cellulose conversion at light intensity of 0.7 W cm^{-2}. Hydrolysis of cellulose to glucose and subsequent formation of HMF were observed under light irradiation with different light intensities. The yield of LeA could be neglected (Fig. S2). The yield of glucose and HMF at light intensity of 0.7 W cm^{-2} demonstrated the highest efficiency; achieving a total conversion of 69.8% at 130 °C for 24 hours. The reaction rate at lower light intensity, such as at 0.5 W cm^{-2} and 0.3 W cm^{-2}, showed relative low conversions of 34.4% and 29.8%, respectively (Fig. S2). The reaction conditions were 50 mg cellulose, 50 mg catalyst, 500 mg water, 4.5 g EMIMCl, at 130 °C for 24 hours.

Section 2: Mechanism of converting glucose to HMF.

The subsequent conversion from glucose to HMF went through a dehydration process with solid acid catalysts (see Scheme S1). Apart from the solid acid (proton H^+) attacking the O in C-O-C (step I in Scheme S1), the glucose went through an opening-cycle reaction. Meanwhile, a carbonyl bond is formed (step II in Scheme S1), which could be enhanced by

plasmonic structure (Au-NPs) and had been well documented by our previous works as well as other groups. To make it simple, this process to form a carbonyl bond could be regarded as a photocatalytic oxidation using plasmonic Au-NPs. [s2,s3] Subsequently, the continuous inter-molecular dehydration processes proceeded. After losing 3 water molecules in total (steps II-IV in Scheme S1), the HMF could be formed. During this process, both acid strength and LSPR effect played crucial roles.

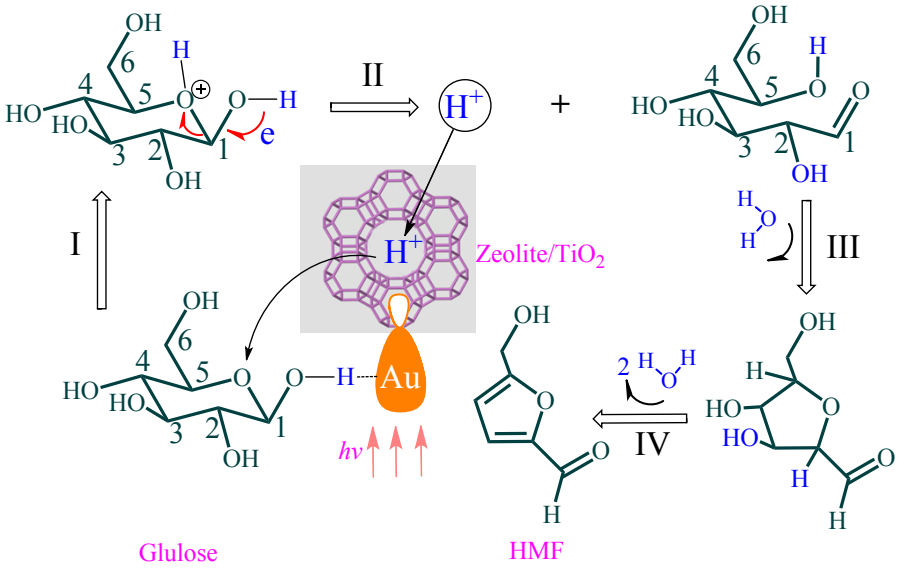

Scheme S1 The processing mechanism for the conversion of glucose to HMF under light irradiation on Au-HYT.

Section 3: Investigations on glass filter with different wavelength ranges.

The light wavelength was also investigated using glass filters to block photons with wavelengths below the filter threshold. For example, the cut-off wavelength of 400 nm means that a majority of the light with wavelength smaller than 400 nm was blocked. Figure S3 showed that the light wavelength ranges of different glass filters, corresponding to the cut-off wavelength of 400 nm, 450 nm, 500 nm and 600 nm, respectively.

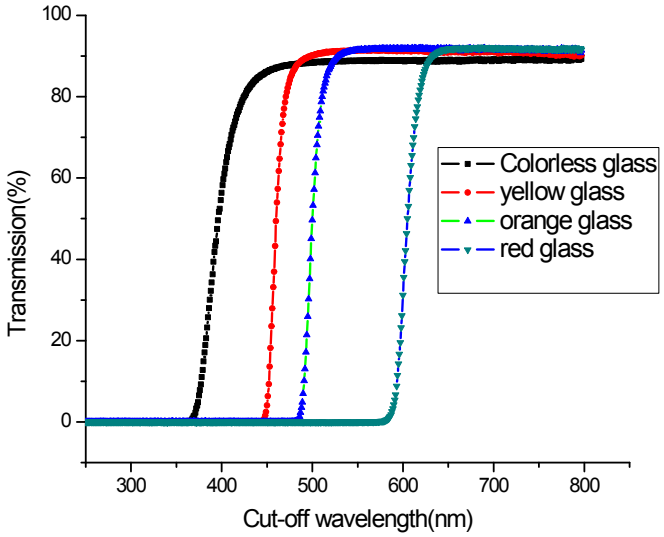

Fig. S3 Investigations on glass filter with different wavelength ranges.

Section 4: Investigations on the catalysts after recycling uses.

This Communication highlighted that a plasmon-enhanced photocatalytic conversion. The morphology of catalysts is not the key point. It will not go through serious changes because the crystlline materials (gold nanoparticles, TiO_2 nanofibres, and zeolites) are very stable after recycling uses in our experimental conditions. The general XRD and SEM characterisations could not identify the tiny differences (if have) with original illustrations shown in Scheme 1 and Figure 1. From the TEM image below (Fig. S4), the 5 nm of Au-NPs, 100 nm of zeolites, and fibrous TiO_2 can be cleanly seen without obvious aggregations or deformations.

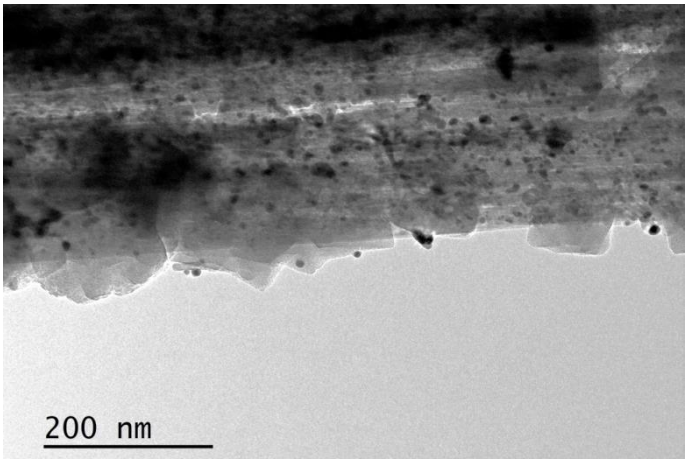

Fig. S4 A TEM image of Au-NPs decorated H-form zeolite Y on TiO_2 NFs after recycling uses.

Reference

S1 X. B. Ke, X. G. Zhang, H. W. Liu, S. Xue, H. Y. Zhu, Efficient catalysts of zeolite nanocrystals grown with a preferred orientation on nanofibers. *Chem. Commun.* 2013, **49**, 9866-9868.

S2 X. G. Zhang, X. B. Ke, A. Du, H. Y. Zhu, Plasmonic nanostructures to enhance catalytic performance of zeolites under visible light, *Sci. Rep.*, 2014, **4**, 3805; X. Zhang, A. Du, H. Zhu, J. Jia, J. Wang, X. B. Ke, Surface plasmon-enhanced zeolite catalysis under light irradiation and its correlation with molecular polarity of reactants, *Chem. Commun.*, 2014, **50**, 1389-1391.

S3 S. I. Naya, A. Inoue, H.Tada, Visible-Light Activity Enhancement of Gold-Nanoparticle-Loaded Titanium(IV) Dioxide by Preferential Excitation of Localized Surface Plasmon Resonance, *ChemPhysChem*. 2011, **12**, 2719-2723; G. Baffou, R. Quidant, Nanoplasmonics for chemistry, *Chem. Soc. Rev*., 2014, **43**, 3898-3907; T. T. Jiang, C. C. Jia, L.C. Zhang, S. R. He, Y. H. Sang, H. D. Li, Y. Q. Li, X. H. Xu, H. Liu, Gold and gold-palladium alloy nanoparticles on heterostructured TiO_2 nanobelts as plasmonic photocatalysts for benzyl alcohol oxidation, *Nanoscale*, 2015, **7**, 209-217.